

Dual-polarization C-band weather radar algorithms for rain rate estimation and hydrometeor classification in an alpine region

H. Paulitsch, F. Teschl, and W. L. Randeu

Department of Broadband Communications, Graz University of Technology, Graz, Austria

Received: 15 September 2008 – Revised: 2 February 2009 – Accepted: 25 February 2009 – Published: 9 March 2009

Abstract. Dual polarization is becoming the standard for new weather radar systems. In contrast to conventional weather radars, where the reflectivity is measured in one polarization plane only, a dual polarization radar provides transmission in either horizontal, vertical, or both polarizations while receiving both the horizontal and vertical channels simultaneously. Since hydrometeors are often far from being spherical, the backscatter and propagation are different for horizontal and vertical polarization. Comparing the reflected horizontal and vertical power returns and their ratio and correlation, information on size, shape, and material density of cloud and precipitation particles can be obtained. The use of polarimetric radar variables can therefore increase the accuracy of the rain rate estimation compared to standard $Z-R$ relationships of non-polarimetric radars. It is also possible to derive the type of precipitation from dual polarization parameters, although this is not an easy task, since there is no clear discrimination between the different values. Fuzzy logic approaches have been shown to work well with overlapping conditions and imprecisely defined class output.

In this paper the implementation of different polarization algorithms for the new Austrian weather radar on Mt. Valluga is described, and first results from operational use are presented. This study also presents first observations of rain events in August 2007 during the test run of the radar. Further, the designated rain rate estimation and hydrometeor classification algorithms are explained.

1 Introduction

In summer 2006, the fifth Austrian C-band weather radar was installed to improve the measurement of rain in the western part of Austria. It is located on Mt. Valluga at 2809 m ASL at the border between the provinces Vorarlberg and Tyrol. The radar is operated by Austro Control, the Austrian air navigation services provider. As opposed to the existing radars, this radar is equipped with dual polarization capabilities.

The Valluga Weather radar is an EEC SidPol version. It is equipped with an ortho-mode feed and electronically controlled waveguide signal routing to provide transmission in either horizontal, vertical, or both polarizations, while receiving both the horizontal and vertical channels simultaneously by two separate receive chains. A mode change from simultaneous transmission to either vertical or horizontal transmission is required for Linear Depolarization Rate (LDR) measurement. The characteristics of the radar are summarized in Table 1.

Dual polarization radars transmit horizontally and vertically polarized electromagnetic pulses and measure the respective reflected powers. By comparing the reflected horizontal and vertical power returns and their ratio and correlation, information on the type, size and shape of cloud and precipitation particles can be obtained. In comparison with a conventional radar system dual polarization systems provide additional fundamental variables:

1.1 Differential reflectivity Z_{DR}

Differential reflectivity is the ratio of the horizontal and vertical power returns. Z_{DR} provides information about particle properties, such as the shape of rain drops. If the majority of the particles in the measured radar volume have a non-spherical shape, and polarization is aligned with the particle axes, the power return will be greater for one polarization than for the other. For large rain drops with an oblate shape,



Correspondence to: H. Paulitsch
(helmutp@radar.tugraz.at)

Table 1. Characteristics of the Valluga radar during test run.

Altitude	2809 m (m.s.l.)
Frequency	5.625 GHz
Beamwidth	0.95° H/0.9° V
Transmitter type	Coaxial magnetron
Peak power	250 kW
Pulse length	0.8 μ s
Pulse repetition rate	1000 s ⁻¹
Samples per integration	50
Rotation rate	4 RPM (24°/sec)
Range resolution	125 m
Number of range-gates	960
Maximum range	120 km
Elevation angles	14 from -1.8° to +90° (-1.8, -0.8, -0.1, 1.0, 2.0, 2.8, 4.2, 7.7, 10.2, 13.7, 19.7, 30.2, 60.0, 90.0)

the horizontal power return will be greater than for the vertical and therefore the Z_{DR} value will be positive (expressed in dB). Small rain drops or light hail particles are more like spherical and result in Z_{DR} values near one or zero dB. Negative dB values can occur for large hail.

1.2 Correlation coefficient ρ_{HV}

The correlation coefficient, ρ_{HV} , is a measure of the correlation between the reflected horizontal and vertical power returns. Generally in rain the correlation is high and ρ_{HV} is close to one. In regions where there is a mixture of precipitation types, such as rain and snow, or where the particle properties are highly irregular, the correlation is much lower and can result in ρ_{HV} values down to 0.8 for example for wet snow.

1.3 Differential phase shift ϕ_{DP}

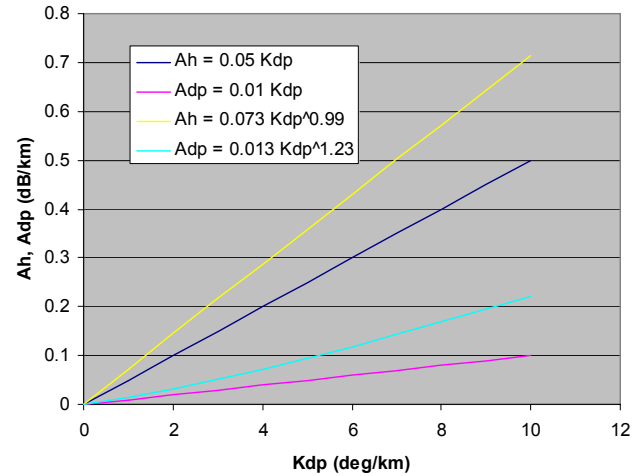
The differential phase shift, ϕ_{DP} , is the phase shift that occurs between the horizontally- and vertically- polarized pulses along the propagation path. The phase shift is caused by variations in the wave propagation speed, when the electromagnetic pulses encounter precipitation particles of different sizes and shapes.

1.4 Specific differential phase K_{DP}

The specific differential phase, K_{DP} , is the range derivative of the differential phase ϕ_{DP} . Since the phase shift is influenced by propagation effects like attenuation or beam shielding, which reduce the power return, it can be used for attenuation correction. K_{DP} is also a good estimator of rain rate.

1.5 Linear depolarization ratio LDR

LDR is the ratio of the cross-polar to the co-polar power return from a horizontally or a vertically polarized pulse. It is

**Fig. 1.** Attenuation correction estimators for C-band.

sensible to particle orientation and canting and is also a good indicator of regions where a mixture of precipitation types occurs or ground clutter is present.

2 Attenuation correction

At C-band wavelength, the attenuation along the propagation path due to precipitation particles can degrade radar measurements to a considerable degree. In order to make accurate rainfall estimates, an attenuation correction scheme for Z_H (Horizontal Reflectivity) and Z_{DR} should be used. The attenuation factors A_H and A_{DP} can be calculated using different methods depending on the type of measurements involved. Studies from Bringi et al. (1990) and Smyth and Illingworth (1998) show different correction methods. Typically methods using the specific differential phase (K_{DP}) are applied. The following relations from Bringi and Chandrasekhar (2001) show a nearly linear relation between attenuation and K_{DP} :

$$A_H = 0.073 K_{DP}^{0.99} \quad (1)$$

$$A_{DP} = 0.013 K_{DP}^{1.23} \quad (2)$$

where A_H is the specific attenuation in dB/km for horizontal polarization, A_{DP} is the specific differential attenuation in dB/km and K_{DP} is the specific differential phase in deg/km.

A_H and A_{DP} are calculated for every radar volume element. The resulting attenuation on a certain path is the sum of all attenuation factors (in dB) along the path. The horizontal reflectivity Z_H and the differential reflectivity Z_{DR} are then raised by the respective values. Such iterative approaches can sometimes be unstable and can lead to unrealistically high reflectivity values. Therefore a simpler approach using linear estimators for attenuation and differential attenuation is used for the Valluga radar. The linear relationship

also allows calculating the attenuation at a certain range-gate directly from the differential phase shift:

$$A_H = 0.05 K_{DP} \quad (3)$$

$$A_{DP} = 0.01 K_{DP} \quad (4)$$

These correction factors are among the lowest that are found in literature. This cautious approach was chosen since the radar operates in a height where mixed phase or solid precipitation is likely to occur. The different correction factors are compared in Fig. 1.

3 Rain rate estimation

Rain rate estimation is one of the main operational applications of weather radars. The use of polarimetric radar variables is expected to increase the accuracy of the rain rate estimation compared to the standard $Z-R$ relationship for non-polarimetric radars, since polarimetric radars can provide a more accurate description of the target. In addition to the horizontal reflectivity (Z_H), especially the specific differential phase (K_{DP}) and the differential reflectivity (Z_{DR}) are applied in rain rate algorithms of polarimetric weather radars. A detailed evaluation of these rainfall algorithms is given by Bringi and Chandrasekhar (2001). The typical form of these estimators is given below:

$$R(K_{DP}) : R = a K_{DP}^b \quad (5)$$

$$R(K_{DP}, Z_{DR}) : R = c K_{DP}^a 10^{(0.1bZ_{DR})} \quad (6)$$

$$R(Z_H, Z_{DR}) : R = c Z_H^a 10^{(0.1bZ_{DR})} \quad (7)$$

where R is the rain rate.

In a previous study (Teschl et al., 2008), polarimetric radar variables were simulated for S-, C- and X-band wavelengths in order to establish radar rainfall estimators for the alpine region of the form $R(K_{DP})$, $R(Z_H, Z_{DR})$, and $R(K_{DP}, Z_{DR})$. For the simulation, drop size distributions of hundreds of 1-minute-rain episodes were obtained from 2D-Video-Distrometer measurements in the mountains of Styria, Austria. Also the influence of different rain drop shape models was investigated. When assuming the model of Brandes et al. (2002) the C-band rain rate estimation algorithms are

$$R(K_{DP}) : R = 18.77 K_{DP}^{0.769} \quad (8)$$

$$R(K_{DP}, Z_{DR}) : R = 22.4 K_{DP}^{0.77} 10^{-0.072 Z_{DR}} \quad (9)$$

$$R(Z_H, Z_{DR}) : R = 0.015 Z_H^{0.82} 10^{-0.290 Z_{DR}} \quad (10)$$

with R in mm/h, K_{DP} in $^{\circ}$ /km, Z_H in $\text{mm}^6 \text{m}^{-3}$ and Z_{DR} in dB.

It is intended to use these estimators in combination with the attenuation correction method described above and to verify the results with ground based observations.

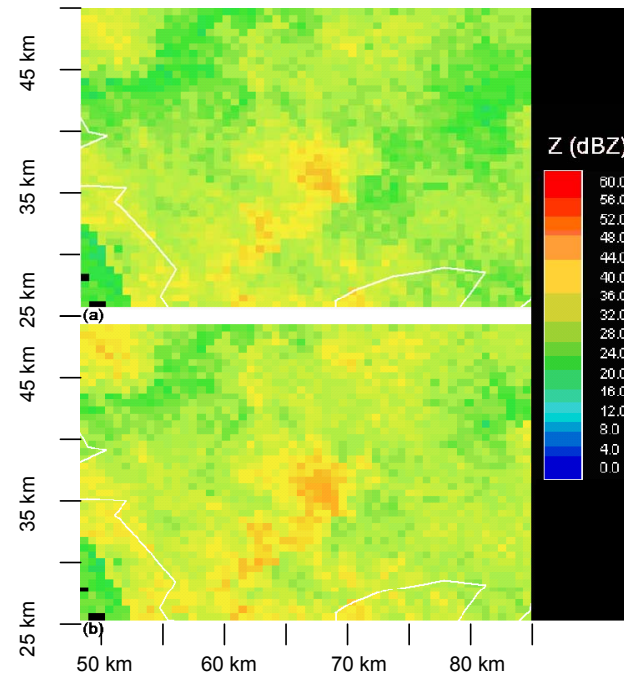


Fig. 2. Reflectivity Z_H of a rain cell seen from the Valluga radar (a) without attenuation correction (b) with attenuation correction $A_H=0.05 K_{DP}$.

4 Hydrometeor classification

For the automatic hydrometeor type classification of the Valluga radar a classification scheme based on fuzzy logic is implemented. Fuzzy logic has several advantages over a Boolean approach, since it can manage to classify in the presence of imprecisely defined class output and cope well with overlapping conditions. The implementation for the Valluga radar is based on the CSU scheme for S-band (Liu, and Chandrasekar, 2000; Lim et al., 2005) with adaptations for C-band weather radars (L. Baldini, personal communication, 2007).

The first step in the classification process is the fuzzification of the input parameters. For the radar parameters Z_H , Z_{DR} , ρ_{HV} , K_{DP} and LDR as well as for the altitude of the observation, membership functions are defined for each of the different hydrometeor types. They are in general beta functions of the form:

$$\beta(x, m, a, b) = \frac{1}{1 + \{[(x - m) / a]^2\}^b} \quad (11)$$

The beta membership functions map an input value x to an output value in the range of $[0, 1]$. The parameters have the following meaning: m locates the centre of the curve while a and b define the width and the slope.

An example of beta membership functions for Z_H is shown in Fig. 3. There are similar functions for LDR , ρ_{HV} and the height. For Z_{DR} and K_{DP} two-dimensional functions are used, since these parameters are dependent on Z_H .

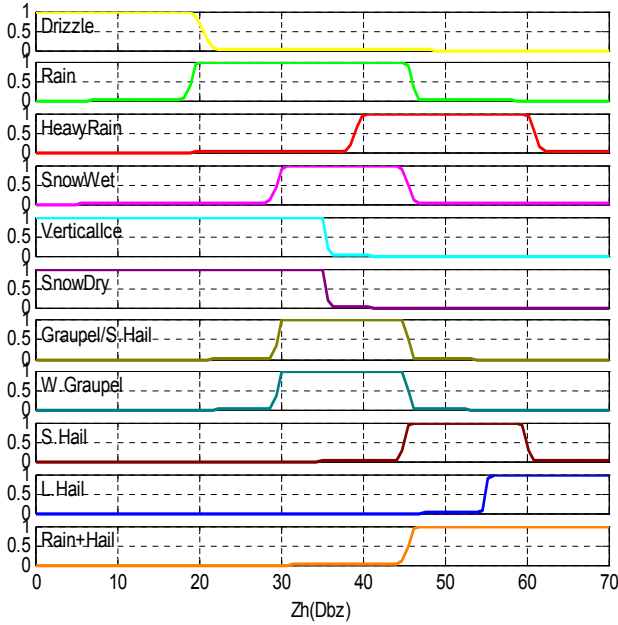


Fig. 3. Membership functions for Z_H (Baldini, 2007).

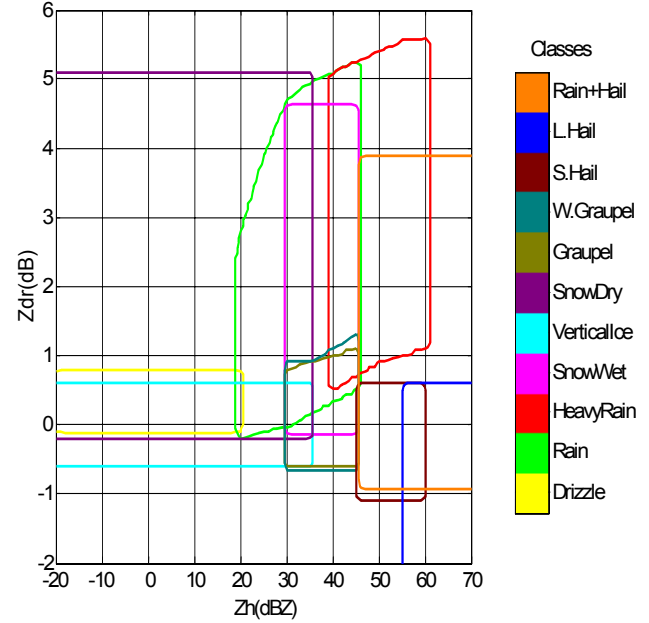


Fig. 4. Membership functions for Z_{DR} and Z_H (Baldini, 2007).

Figure 4 shows an example of two-dimensional functions for Z_{DR} and Z_H (Baldini, 2007).

For a set of given input parameters the most likely hydrometeor type is the one with the highest rule strength value. The rule strength is defined as:

$$R_j = \mu_j^{Z_H}(Z_H) \times \mu_j^H(Height) \times \left[\begin{array}{l} w_j^{Zdr} \mu_j^{Zdr}(Zdr) + w_j^{Kdpr} \mu_j^{Kdpr}(Kdp) + \\ w_j^{LDR} \mu_j^{LDR}(LDR) + w_j^{\rho_{hv}} \mu_j^{\rho_{hv}}(\rho_{hv}) \end{array} \right] \quad (12)$$

where μ are the beta functions and w are weight factors.

Eleven hydrometeor types including drizzle, light and heavy rain, dry and wet snow, and different intensities of graupel and hail are defined.

5 Results

The radar started routine operation in October 2007, using single polarization only. In a test phase before this time several dually polarized measurements have been collected. Unfortunately no LDR scans were available and also the K_{DP} parameter was not calculated by the radar software. Therefore it was not possible to test the K_{DP} based rain rate estimators. Without these parameters also the fuzzy logic classification scheme must make decisions based on fewer inputs, which consequently leads to a higher variance.

The radar images below show a precipitation event with mostly wide spread precipitation, on 29 August 2007 at 10:37 local time. During this event reflectivity values up to 48 dBZ were measured in some embedded cells in the north-eastern part of the image (Fig. 5). All figures show a constant

altitude plan position indicator (CAPPI) at a height of 2.5 km and a vertical cross section along the line indicated in Fig. 5a.

Figures 6, 7 and 8 show the differential reflectivity Z_{DR} , the correlation coefficient ρ_{HV} and the differential phase ϕ_{DP} , respectively. For a large area in the vertical cross section no ρ_{HV} and ϕ_{DP} parameters are available. This causes also the hydrometeor classification to fail in this area.

The result of the classification is shown in Fig. 9. The hydrometeor classification indicates dry and wet snow, rain and wet graupel in the CAPPI. In the vertical cross section dry snow is the predominant hydrometeor type above 4 km, which changes to heavy rain, wet snow, wet graupel and rain+hail below.

An example for the attenuation correction of a rain cell for the reflectivity factor Z_H is shown in Fig. 2. Even with these low correction factors, differences of about 3 dB between the corrected and the uncorrected data can be seen. A certain radar beam at an elevation of -0.1° and an azimuth of 56° degrees through this area has been further analyzed. The profile of the polarization parameters along the beam can be seen in Fig. 10. Figure 11 compares the attenuated with the corrected reflectivity. The parameters are averaged over four range gates to give the same 500 m resolution as in Fig. 2. Even with this range-averaging the noise in ϕ_{DP} is quite large, especially for ranges beyond 50 km. Z_{DR} also shows rather large positive values with a mean value around 4 dB.

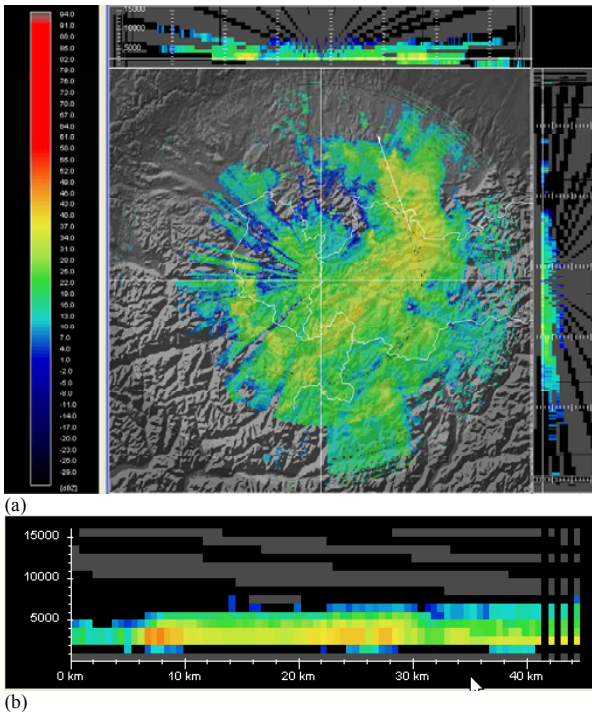


Fig. 5. Z_H (dBZ), 29 August 2007, 10:37 (a) CAPPI 2.5 km (b) Vertical cross section.

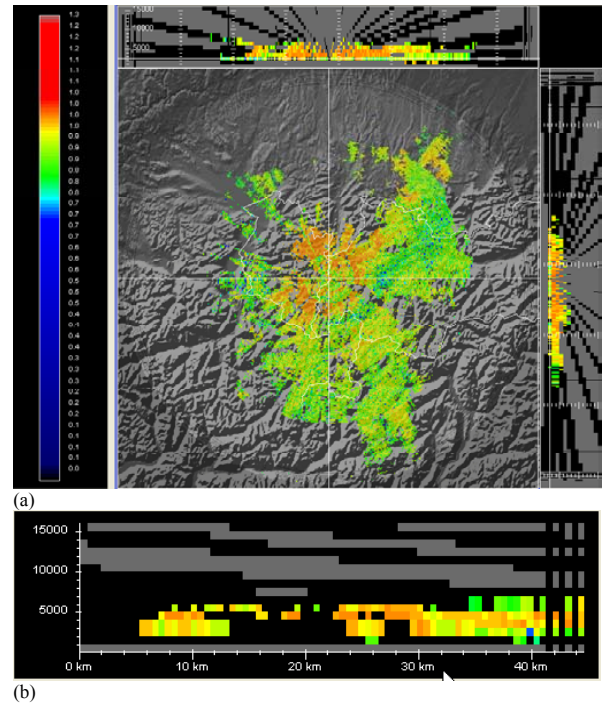


Fig. 7. ρ_{HV} , 29 August 2007, 10:37 (a) CAPPI 2.5 km (b) Vertical cross section.

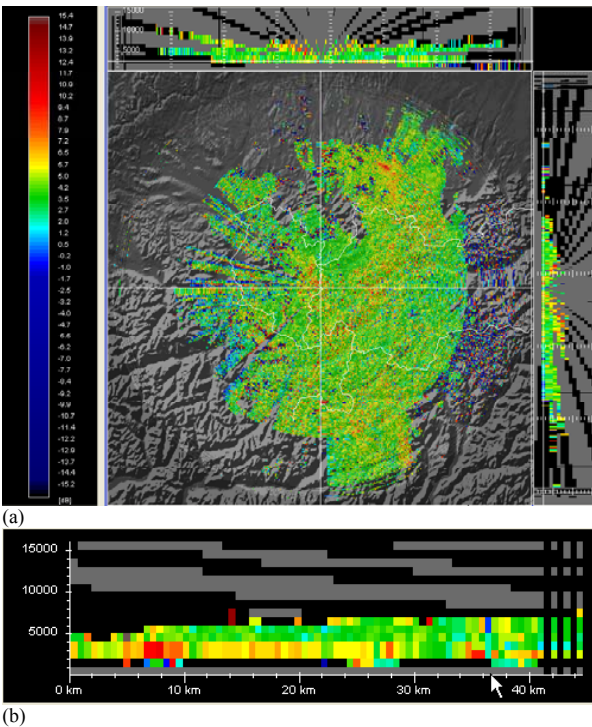


Fig. 6. Z_{DR} (dB), 29 August 2007, 10:37 (a) CAPPI 2.5 km (b) Vertical cross section.

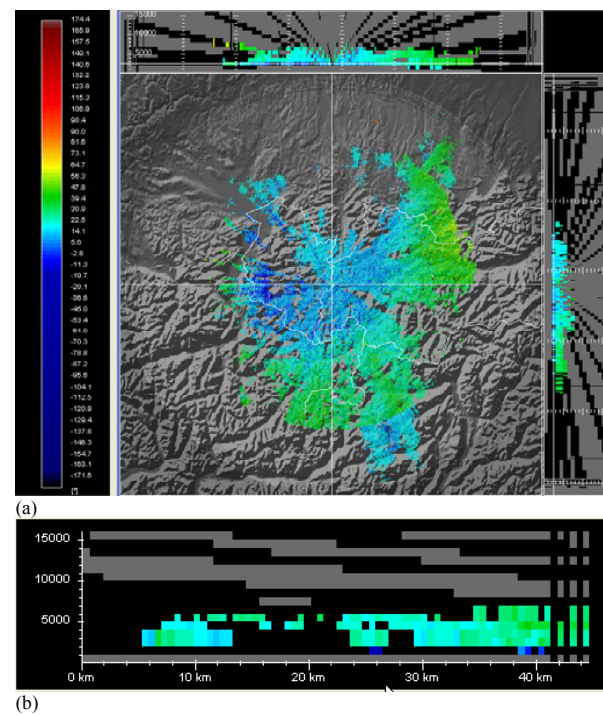


Fig. 8. ϕ_{DP} (deg), 29 August 2007, 10:37 (a) CAPPI 2.5 km (b) Vertical cross section.

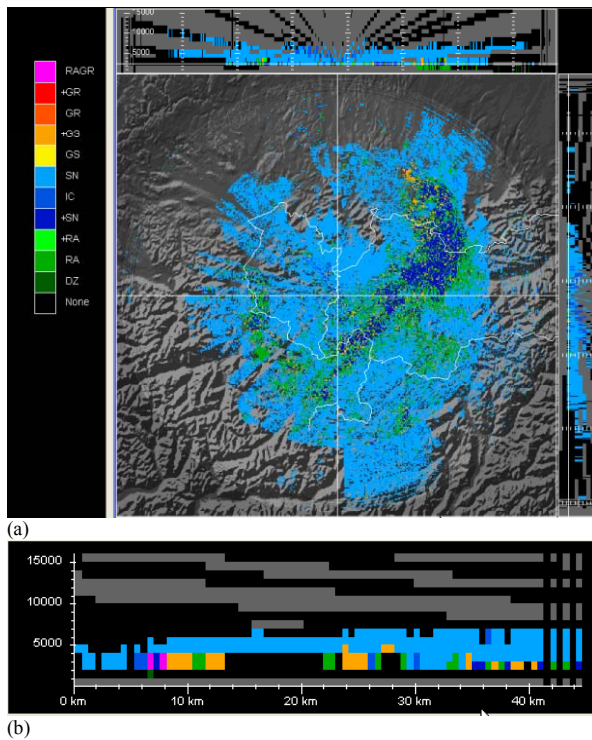


Fig. 9. Hydrometeor classification, 29 August 2007, 10:37 (a) CAPPI 2.5 km (b) Vertical cross section (RAGR: rain and hail, +GR: large hail, GR: hail, +GS: wet graupel, GS: graupel, SN: snow, IC: ice, +SN: wet snow, +RA: heavy rain, RA: rain, DZ: drizzle).

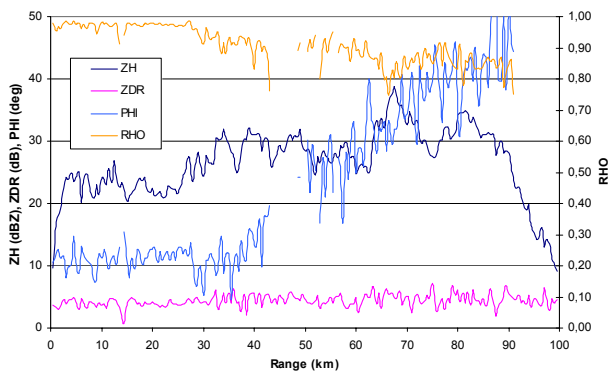


Fig. 10. Radar parameters along a single ray (azimuth 56° , elevation -0.1°).

6 Conclusion and outlook

This study presents first observations of precipitation events during the test run of the Valluga C-band weather radar. Since the radar is located at more than 2800 m ASL, precipitation often occurs in solid or in mixed phase form. First promising results of the classification algorithm have shown the occurrence of different hydrometeor types like graupel, rain and snow, which is the predominant precipitation type

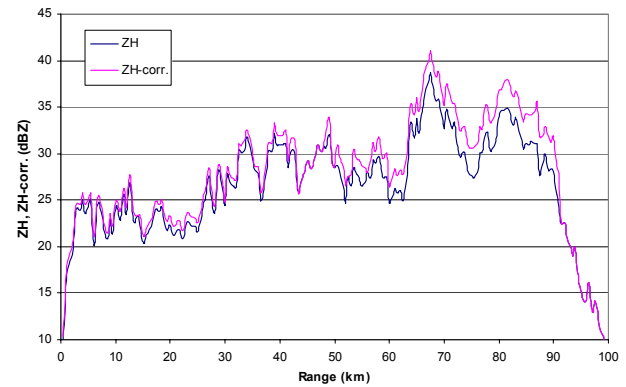


Fig. 11. Effect of attenuation correction on Z_H along a single ray (azimuth 56° , elevation -0.1°).

at this height. An important future step will be to adjust the current hydrometeor classification parameters (membership functions and weight factors) for reliable use in the alpine region.

Acknowledgement. The authors gratefully acknowledge the provision of Valluga weather radar data by Austro Control, the Austrian air navigation services provider (Dept. of Aviation Meteorology, Mr. Kaltenböck).

Edited by: S. C. Michaelides

Reviewed by: two anonymous referees

References

- Baldini, L., Gorgucci, E., Chandrasekar, V., and Peterson, W.: Implementations of CSU hydrometeor classification scheme for C-band polarimetric radars, 32nd Conference on Radar Meteorology, September 2005, Albuquerque, NM 2005.
- Brandes, E., Zhang, G., and Vivekanandan, J.: Experiments in rainfall estimation with a polarimetric radar in a subtropical environment, *J. Appl. Meteor.*, 41, 674–685, 2002.
- Bringi, V. N. and Chandrasekar, V.: Polarimetric Doppler Weather Radar. Principles and Applications. Cambridge University Press, NY, 636 pp., 2001.
- Lim, S., Chandrasekar, V., and Bringi, V. N.: Hydrometeor Classification System Using Dual-Polarization Radar Measurements: Model Improvements and In Situ Verification, *IEEE Trans. Geosci. Remote Sens.*, 43, 792–801, 2005.
- Liu, H., and Chandrasekar, V.: Classification of Hydrometeors Based on Polarimetric Radar Measurements: Development of Fuzzy Logic and Neuro-Fuzzy Systems, and In Situ Verification, *J. Atmos. Oceanic Technol.*, 17, 140–164, 2000.
- Smyth, T. J. and Illingworth, A. J.: Correction for attenuation of radar reflectivity using polarization data, *Quart. J. Roy. Meteor. Soc.*, 124, 2393–2415, 1998.
- Teschl, F., Randeu, W. L., Schönhuber, M., and Teschl, R.: Simulation of polarimetric radar variables in rain at S-, C- and X-band wavelengths, *Adv. Geosci.*, 16, 27–32, 2008, <http://www.adv-geosci.net/16/27/2008/>.